

AD-A209 153



A METHODOLOGY FOR MODELING
RADAR DETECTION RANGE IN
AIR COMBAT SIMULATION

THESIS

Damon Neal Lum
Major, USAF

AFTT/GST/ENS/89M-12

DTIC
SELECTE
JUN 20 1989
SCE D

DEPARTMENT OF THE AIR FORCE
AIR UNIVERSITY

AIR FORCE INSTITUTE OF TECHNOLOGY

Wright-Patterson Air Force Base, Ohio

This document has been approved
for public release and sale; its
distribution is unlimited.

89 6 19 075

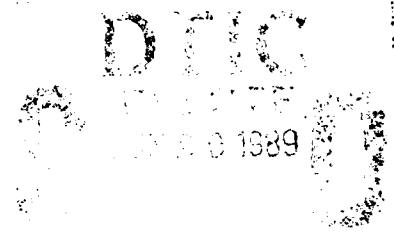
AFIT/GST/ENS/89M-12

A METHODOLOGY FOR MODELING
RADAR DETECTION RANGE IN
AIR COMBAT SIMULATION

THESIS

Damon Neal Lum
Major, USAF

AFIT/GST/ENS/89M-12



Approved for public release; distribution unlimited

A METHODOLOGY FOR MODELING
RADAR DETECTION RANGE IN
AIR COMBAT SIMULATION

THESIS

Presented to the Faculty of the
of the Air Force Institute of Technology
Air University
In Partial Fulfillment of the
Requirements for the Degree of
Master of Science in Operations Research

Damon Neal Lum, B.S., M.S.

Major, USAF

March, 1989



Accession For	
NTIS GRA&I	<input checked="" type="checkbox"/>
DTIC TAB	<input type="checkbox"/>
Unannounced	<input type="checkbox"/>
Justification	
By _____	
Distribution/	
Availability Codes	
Dist	Avail and/or Special
A-1	

Approved for public release; distribution unlimited

Preface

Radar detection range models used in air combat simulations impact the accuracy and required run time of the computer simulation. User requirements will establish a compromise between accuracy of the detection range model and the required run time for the simulation. This thesis provides a method to predetermine the radar detection range for fighter aircraft given specific intercept scenarios.

I want to thank the members of my thesis committee, Lt Col Thomas Schuppe and Lt Col David Meer. They helped me overcome the significant challenges I faced in this research project. I also want to thank, Lt Col Ron Browning, AFCSA/SAGF, for sponsoring the thesis topic. Mr. Frank Campanile, ASD/ENSSE, provided outstanding support for needed data from TAC BRAWLER. A special thanks goes to Mr. Larry Taranto who gladly gave assistance in running TAC BRAWLER to generate the needed data and answered my numerous questions. I also thank Maj Ken Bauer for his time and expertise on response surface methodology.

Finally, I am deeply in debt to my family, especially my wife Diane. With our youngest of three sons born one week before finals of the first quarter, things at home were very busy. The accomplishment of this effort is greatly due to Diane's support.

Damon Neal Lum

Table of Contents

	Page
Preface	ii
Table of Contents	iii
List of Figures	vi
List of Tables	vii
List of Symbols	viii
Abstract	xi
I. INTRODUCTION	1-1
1.1 Background	1-1
1.2 Model Requirements	1-3
1.3 Problem Statement	1-4
1.4 Research Question	1-4
1.5 Research Objective	1-4
1.6 Scope	1-4
1.7 Assumptions	1-5
1.8 Overview	1-5
II. LITERATURE SEARCH	2-1
2.1 Overview	2-1
2.2 Radar Principle	2-1
2.3 Predicting Detection Range	2-2
2.3.1 Signal-to-Noise Ratio.	2-2
2.3.2 Signal-to-Clutter Ratio.	2-6

	Page
2.3.3 Detectability Factor.	2-9
2.4 TAC BRAWLER Air Combat Model	2-10
2.4.1 TAC BRAWLER's Radar Model.	2-10
2.4.2 Using TAC BRAWLER to Determine Radar Detection Range.	2-11
2.5 Summary	2-12
III. METHODOLOGY	3-1
3.1 Overview	3-1
3.2 Closed Form Equations	3-1
3.3 Response Surface Methodology	3-4
3.3.1 Predictors.	3-5
3.3.2 Predictor Levels.	3-5
3.3.3 Experimental Design and Replications.	3-5
3.4 Selecting the Best Regression Equation.	3-6
3.5 Incorporating the Solution	3-9
IV. RESULTS	4-1
4.1 TAC BRAWLER Results	4-1
4.2 Regression Results	4-2
V. CONCLUSIONS AND RECOMMENDATIONS	5-1
5.1 Conclusions	5-1
5.2 Recommendations	5-2
5.2.1 Applications.	5-2
5.2.2 Future Research.	5-3
Appendix A. CLOSED FORM SOLUTION	A-1
A.1 Intercept Geometry	A-1
A.2 Solving for $\tan \psi$ in Terms of R_c	A-3

	Page
A.3 Solving for R in Terms of R_c	A-4
A.4 Single Variable Range Equation	A-5
Appendix B. TAC BRAWLER DATA	B-1
Appendix C. TEST POINT DATA	C-1
Appendix D. SAS DATA	D-1
D.1 SAS MAXR Program File	D-1
D.2 SAS MAXR Output	D-2
D.3 ANOVA and Residual Plots	D-10
Bibliography	BIB-1
Vita	VITA-1

List of Figures

Figure	Page
3.1. Angles of Incidence	3-1
3.2. Attacker and Target Geometry	3-2
3.3. Attacker and Horizon Geometry	3-3
A.1. Intercept Geometry	A-1

List of Tables

Table	Page
3.1. Predictor Values and Levels	3-5
3.2. Fractional Design for Experimental Runs	3-6
3.3. Test Point Values and Levels	3-8
4.1. Mallows C_p Statistic Summary	4-2
4.2. Validation Results	4-3

List of Symbols

Symbol	Page
S	2-2
N	2-2
P_t	2-3
R	2-3
I_i	2-3
G_t	2-3
I_m	2-3
I_t	2-3
σ	2-3
I_r	2-3
S_f	2-3
A_r	2-3
λ	2-4
F	2-4
L_t	2-4
L_α	2-4
T_s	2-4
B_n	2-4
k	2-4
τ	2-5
F_s	2-5
P_{avg}	2-6
$R_{s/n}$	2-6
k_r	2-6
σ_c	2-7

Symbol	Page
F_c	2-7
R_c	2-7
L_{am}	2-7
C	2-7
γ	2-7
ψ	2-7
A_c	2-7
θ_a	2-7
L_p	2-7
τ_n	2-7
c	2-7
S/C	2-8
I_d	2-8
$R_{s/c}$	2-8
k_c	2-8
$D_x(n)$	2-9
x	2-9
$D_0(1)$	2-9
n	2-9
$L_i(n)$	2-9
$L_f(N)$	2-9
$D_1(n)$	2-9
I_n	2-9
S_n	2-10
G_{mb}	2-11
L_{mb}	2-11
ϕ_t	3-2

Symbol	Page
ϕ_h	3-2
R_e	3-2
A_h	3-2
T_h	3-2
RSS_p	3-7
p	3-7
n	3-7
s^2	3-7
k_t	A-4

Abstract

The purpose of this thesis is to develop a methodology for modeling fighter aircraft radar detection range performance. Response surface methodology is used to form a meta-model of the TAC BRAWLER Air Combat Model. Using experimental design theory, detection range data was collected using TAC BRAWLER and regressed to develop an equation for predicting radar detection range. The resulting equation is valid for specific ranges of the target's radar cross section, altitude, and airspeed and the attacker's altitude and airspeed.

A METHODOLOGY FOR MODELING RADAR DETECTION RANGE IN AIR COMBAT SIMULATION

I. INTRODUCTION

1.1 Background

The intercept phase of air-to-air combat begins with the radar detection of adversary aircraft. The intercept phase ends and the engagement phase begins when weapons can be employed against the adversary aircraft (1:139). Longer radar detection ranges provide the additional time required to employ intercept tactics developed for higher probabilities of success. Shorter radar detection ranges provide less lead time and may force the use of less effective tactics. As a result, radar detection range dictates the intercept tactic selected and influences air-to-air engagement results.

Because air-to-air engagement results are influenced by radar detection range, computer simulations of air-to-air combat must accurately model radar detection range to produce valid engagement results. An inaccurate radar detection range model provides erroneous initial conditions for the geometry of the intercept phase. These erroneous initial conditions could provide false advantages for some aircraft and affect the outcome of simulated air-to-air engagements. Additionally, computer simulations which overestimate detection range could incorrectly simulate engagements in situations where adversary aircraft are beyond the actual detection range and air-to-air combat should not occur. Computer

simulations which underestimate detection range could also fail to simulate engagements that should occur.

Two terms are defined to ease the comprehension of aircraft geometry during the intercept phase. The term, *attacker*, refers to the aircraft searching with radar and the term, *target*, refers to aircraft being searched for. In cases where both aircraft have radar, there are two attacker/target scenarios. Both scenarios would be evaluated to determine which aircraft has the greater radar detection range and would initiate the engagement.

Radar detection range is determined using radar range equations for particular attacker and target positions. As the aircraft positions change, so may the detection range. A common technique in air combat simulation is to continuously track aircraft positions, allowing the radar range equations to be frequently evaluated as the attacker and target approach each other. The radar range equations are iterated to determine the point where the target is within radar detection range of the attacker. A model of this type is referred to as an iterative model. The accuracy of an iterative model for determining detection range is directly proportional to the frequency of the range equation evaluations. However, the higher the frequency of evaluations, the longer the required computer time. Computer simulations of air-to-air combat using an iterative detection range model may be very accurate but extremely slow to run.

Assumptions can be made to significantly reduce the computer time required to determine detection range. For example, if the effects of surface clutter and jammers are ignored and the target's radar cross section is assumed to be constant, the radar detection range will be constant. By ignoring surface clutter and jamming, radar detection range is

a function of the target's radar cross section and the simulation can run without iterating radar range equations. This type of model is referred to as a predetermined detection range model. Using a predetermined radar detection range model, intercepts can be established based on the aircraft flight paths. A predetermined radar detection range model establishes detection range based on the relative distance between the attacker and target.

1.2 Model Requirements

The Air Force Center for Studies and Analyses, Fighter Division (SAGF) is interested in a predetermined detection range model to limit the computer run time of air-to-air combat simulations. However, the radar detection range model must account for surface clutter and the target's aspect dependent radar cross section. The air-to-air combat simulation makes the following assumptions which define the operational environment for the detection range model (2).

1. The radar cross section for targets of interest will range between 1 and 10 square meters.
2. Targets will maintain an altitude between 200 and 1,000 feet above ground level (AGL).
3. Attackers will maintain an altitude between 10,000 and 25,000 feet AGL.
4. Target speeds will be between .580 and .774 Mach.
5. Attacker speeds will be between .676 and .774 Mach.

1.3 Problem Statement

Computer simulations which model radar detection range by iterating radar range equations require too much computer time. Detection ranges calculated by ignoring surface clutter effects are not accurate enough.

1.4 Research Question

How can radar performance be modeled to establish a predetermined detection range which accounts for surface clutter effects?

1.5 Research Objective

The purpose of this research effort is to develop a model for predetermining radar detection range which accounts for surface clutter effects.

1.6 Scope

The radar detection range model developed in this thesis applies to the radar of airborne fighter aircraft searching for airborne fighter targets. The characteristics of the attacker's radar and the target are representative of fighter aircraft and only unclassified data is presented or used in this thesis. The model is developed for only one attacker radar; however, the methodology can be used to model the detection range performance of other radars. The model does not include effects from jamming.

1.7 Assumptions

Although the radar detection range model applies to aircraft at different altitudes and speeds, the model assumes the aircraft altitudes and speeds will not change prior to radar detection. The terrain is assumed to be flat. Assuming flat terrain is required to simplify the calculation of the range to clutter. The model also assumes the radar cross section of the target can be represented by a single value for specific ranges of azimuth and elevation aspect angles. The ground controlled intercept will limit the attacker's position during the intercept. The attacker's position is assumed to be within ± 10 degrees off the target's nose in azimuth. Elevation angles will be limited to ± 60 degrees, the typical gimble limits of fighter radars. The model also assumes the attacker's radar will search the correct azimuth and elevation angles to place the target within the radar search volume.

1.8 Overview

Chapter II presents a brief description of radar operation, the radar range equations used to determine detection range, and TAC Brawler, an air-to-air combat computer simulation. Chapter III describes the methodology used to answer the research question. Chapter IV provides results from the methodology and Chapter V presents conclusions from the research effort and recommendations.

II. LITERATURE SEARCH

2.1 Overview

The term, *RADAR*, is an acronym from the words *R*Adio *D*etection And *R*anging (3:15). As implied by the source words for the acronym, radar uses radio frequency energy to detect and determine the distance to targets. The emphasis of this thesis is radar detection range performance. This chapter provides a brief explanation of the principle of radar, the equations used to predict detection range, a description of TAC BRAWLER an accepted Air Force air-to-air combat computer simulation, and a summary.

2.2 Radar Principle

The basic principle of radar is the use of electromagnetic energy to locate targets. Target detection is possible because the radar radiates pulses of electromagnetic energy which intercept the target and are reradiated back to the attacker. The energy which is reradiated by the target and enters the radar receiver is called the target's *signal*. Complicating the detection process is interference, undesirable electromagnetic energy, which also enters by the radar receiver (4:18). The primary sources for the interference are thermal *noise* and *clutter*. Noise may originate in the receiver or enter with the signal. Clutter is energy reflected from objects the radar is not designed to detect. For a radar designed to map terrain, aircraft will be a source of clutter. In this thesis, the radar is designed to detect aircraft and terrain is the clutter source of concern.

Because of noise and clutter, a minimum energy level or threshold is established for reporting targets. An alarm, target detection, is reported for energy levels above

the threshold. The threshold must be sufficiently high to eliminate false alarms, due to noise and/or clutter, yet low enough to provide an alarm for actual targets (5:175). The threshold value is determined by the specific design of the radar and the value of the *detectability factor*. The *detectability factor* is the minimum signal-to-noise ratio required to detect targets. The value of the *detectability factor* is based on the desired probabilities of detection and false alarm, and assumptions about the fluctuation of the target's signal (6:19).

2.3 Predicting Detection Range

Predictions of radar detection range are determined by setting the *detectability factor* equal to the estimated target *signal-to-noise* ratio. In cases where the interference is dominated by clutter the detection range is determined based on estimates for the *signal-to-clutter* ratio. As a result, the key components for modeling radar detection range are the signal-to-noise ratio, the signal-to-clutter ratio, and the *detectability factor*.

2.3.1 Signal-to-Noise Ratio. The power of the target's signal entering the radar receiver is denoted by S . The equation for S is developed from equations (2.1– 2.7). These equations account for the transmission of power from the attacker's radar, to the target, and back. The noise power, N , is developed from equations (2.8–2.10). The signal-to-noise ratio is the quotient of S divided by N and is given in equation (2.13). These equations were derived from information presented by Barton (6).

For an isotropic antenna, the peak transmit power of the radar is evenly distributed in all directions. The isotropic power density represents the distribution of the peak power

over the surface of a sphere as given by

$$I_i = \frac{P_t}{4\pi R^2} \quad (2.1)$$

where P_t is the peak transmit power in watts, R is the distance from the attacker to the target in meters, and I_i is the isotropic power density in watts per square meter. However, the radar's transmitting antenna is able to focus the direction of the power along the axis of a mainbeam. The power density of the mainbeam is given by

$$I_m = \frac{P_t G_t}{4\pi R^2} \quad (2.2)$$

where G_t is the transmit antenna gain in ratio form and I_m is the power density of the mainbeam in watts per square meter.

The transmitted power intercepted by the target, I_t , is the product of the power density of the mainbeam, I_m , and the target's radar cross section, σ . The equation for I_t is

$$I_t = I_m \sigma = \frac{P_t G_t \sigma}{4\pi R^2} \quad (2.3)$$

where σ is the radar cross section of the target in square meters and I_t is the power intercepted by the target in watts. The power intercepted by the target is isotropically radiated. Again, the power will be distributed over the surface of a sphere. The power density will be

$$I_r = \frac{I_t}{4\pi R^2} = \frac{P_t G_t \sigma}{(4\pi R^2)^2} \quad (2.4)$$

where I_r is the power density radiated from the target in watts per square meter.

The power entering the attacker's radar, S_f , is the product of the power density reradiated from the target, I_r , and the receiving antenna aperture, A_r . The equation for

A_r is

$$A_r = \frac{G_r \lambda^2}{4\pi} \quad (2.5)$$

where G_r is the receiving antenna gain in ratio form, λ is the wavelength in meters, and A_r is the receiving antenna aperture in square meters. The equation for S_f becomes

$$S_f = I_r A_r = \frac{P_t G_t G_r \lambda^2 \sigma}{(4\pi)^3 R^4} \quad (2.6)$$

where S_f is power from the target intercepted by the radar antenna in watts. Three factors are applied to S_f to attain S . The equation for S is given by

$$S = \frac{S_f F^4}{L_t L_\alpha} = \frac{P_t G_t G_r \lambda^2 \sigma F^4}{(4\pi)^3 R^4 L_t L_\alpha} \quad (2.7)$$

where F is a pattern-propagation factor to the target in ratio form, L_t is the transmission line loss in ratio form, L_α is atmospheric attenuation to the target in ratio form, and S is the target's signal power entering the radar receiver in watts. The pattern-propagation factor, F , is the ratio of the field strength at a point from a radio transmission (excluding attenuation effects) to the strength of the same system operating in free space (6:288). A value of one is typically used for F (6:44). The transmission line loss, L_t , is radar specific with typical values of about 2 (4:58). Atmospheric attenuation accounts for radar energy losses from absorption in the air and has an L_α value around 1.3 (6:23).

Noise power at the input of the receiver due to thermal energy is given by

$$N = k T_s B_n \quad (2.8)$$

where T_s is the effective system temperature in Kelvins, B_n is the noise bandwidth in Hertz, k is Boltzmann's constant, 1.38×10^{-23} watts per Hertz Kelvin, and N is the noise

power due to thermal energy in watts. Assuming a matched filter, the noise power can be rewritten as

$$N = kT_s \frac{1}{\tau} \quad (2.9)$$

where τ is the transmitted pulsewidth in seconds.

The effective system temperature at the output of the antenna is obtained by multiplying a standard temperature by a factor called the noise figure (4:19). The standard system noise figure, F_s , is the ratio of noise output from the receiver to the noise out of an ideal receiver at standard temperature, $T_0 = 290K$. The noise can then be expressed as

$$N = kF_s T_0 \frac{1}{\tau} \quad (2.10)$$

The signal-to-noise ratio for a single pulse is the quotient from equation (2.7) divided by equation (2.10) as given by

$$S/N = \frac{P_t \tau G_t G_r \lambda^2 \sigma}{(4\pi)^3 R^4 k F_s T_0} \quad (2.11)$$

The radar being modeled in this thesis will sweep the target and many pulses will intercept the target. With multiple returns from the target, the radar is capable of target detection at reduced signal-to-noise ratios. In essence the detectability factor is a fraction of the signal-to-noise ratio. An integration factor, I_n , is used to convert the signal-to-noise factor to a detectability factor. The development of I_n is presented in the detectability factor section of this chapter. For most pulse doppler radars the integration time is $1/B_f$, the inverse of the doppler filter bandwidth. The number of pulses integrated is $1/B_f \times f_r$,

where f_r is the pulse repetition frequency. The equation for signal-to-noise becomes

$$(S/N)I_n = \frac{P_r f_r G_t G_r \lambda^2 \sigma}{(4\pi)^3 R^4 k F_s T_0 B_f} \quad (2.12)$$

$$S/N = \frac{P_{avg} G_t G_r \lambda^2 \sigma}{I_n (4\pi)^3 R^4 k F_s T_0 B_f} \quad (2.13)$$

where P_{avg} is the average power as the result of $P_t \times \tau \times f_r$. For a given signal-to-noise level, the maximum radar detection range based on noise as the dominant source of interference, $R_{s/n}$, can be determined by

$$R_{s/n}^4 = k_r \sigma \quad (2.14)$$

where $R_{s/n}$ is in meters, σ is set by the simulation for the target of interest, and k_r is a radar constant for signal-to-noise as given by

$$k_r = \frac{P_{avg} G_t G_r \lambda^2}{S/N I_n (4\pi)^3 k F_s T_0 B_f} \quad (2.15)$$

Radar detection range limited by noise is easily calculated by equation (2.14).

2.3.2 Signal-to-Clutter Ratio. The power entering the radar receiver due to clutter is calculated in much the same manner as for the target's signal. The important difference is the clutter cross section used to calculate the power intercepted by clutter. Since the intercept is head on and the closing velocity between the attacker and target is higher than the velocity of the radar, the target should fall within a clutter free doppler filter. However, there may be a significant spillover of clutter power into clutter free filters due to the power of the mainbeam. The equation for the power entering the radar receiver due to clutter for a single pulse is given by Barton (6:38) as

$$C = \frac{P_t G_t G_r \lambda^2 \sigma_c F_c^4}{(4\pi)^3 R_c^4 L_t L_{oc}} \quad (2.16)$$

where σ_c is the clutter cross section for the terrain within the resolution cell of the mainbeam in square meters F_c is the pattern-propagation factor to the mainbeam clutter in ratio form, R_c is the range to the clutter in meters, L_{am} is the atmospheric attenuation to the clutter in ratio form, and C is the noise power entering the radar receiver due to clutter in watts.

The clutter cross section is the product of the surface area within the radar resolution cell, the surface clutter reflectivity factor, γ , and the sine of the grazing angle, ψ . The equation for σ_c is given by

$$\sigma_c = A_c \gamma \sin \psi \quad (2.17)$$

where A_c is the surface area within the resolution cell of the mainbeam in square meters, γ is the dimensionless clutter reflectivity factor, and ψ is the grazing angle of the mainbeam in degrees. The surface area within the radar resolution cell of the mainbeam is given by

$$A_c = \frac{R_c \theta_a}{L_p} \frac{\tau_n c}{2} \sec \psi \quad (2.18)$$

where θ_a is the azimuth half-power beamwidth in radians, L_p is the beamshape loss in ratio form, τ_n is the processed pulsewidth in seconds, and c is the velocity of light in meters per second. The value of the surface reflectivity factor is terrain dependent and ranges in value from .03 to .15 (6:42). The equation for σ_c becomes:

$$\sigma_c = A_c \gamma \sin \psi = \frac{R_c \theta_a \tau_n c \gamma \tan \psi}{2 L_p} \quad (2.19)$$

Substituting σ_c into equation (2.16) produces the equation for noise power entering the radar receiver due to mainbeam clutter as

$$C = \frac{P_t G_t G_r \lambda^2 F_c^4 \theta_a \tau_n c \gamma \tan \psi}{2(4\pi)^3 R_c^3 L_t L_{am} L_p} \quad (2.20)$$

The signal-to-clutter ratio due to mainbeam clutter, S/C , can be solved for by dividing equation (2.7) by equation (2.20). The result is

$$S/C = \frac{2R_c^3 L_{\alpha m} L_p F^4 \sigma}{R^4 L_{\alpha} F_c^4 \theta_a \tau_n c \gamma \tan \psi} \quad (2.21)$$

Since the detection ranges typical of fighter radars and fighter targets are well within the radar horizon, $F = F_c$ and $L_{\alpha} = L_{\alpha m}$ are assumed. This simplifies equation (2.21) to

$$S/C = \frac{2R_c^3 L_p \sigma}{R^4 \theta_a \tau_n c \gamma \tan \psi} \quad (2.22)$$

Through doppler filtering, the signal-to-noise can be significantly improved. This improvement is on the order of 10^8 for high pulse repetition frequency radars (6:44). The final equation for signal-to-clutter can be expressed as

$$S/C = \frac{I_d 2R_c^3 L_p \sigma}{R^4 \theta_a \tau_n c \gamma \tan \psi} \quad (2.23)$$

where I_d is the doppler improvement factor in ratio form. For a given signal-to-clutter ratio, the maximum detection range based on clutter as the dominant interference source, $R_{s/c}$, can be computed by

$$R_{s/c}^4 = \frac{k_c \sigma R_c^3}{\tan \psi} \quad (2.24)$$

where $R_{s/c}$ is in meters and k_c is a radar constant for signal-to-clutter as given by

$$k_c = \frac{2I_d L_p}{S/C \theta_a \tau_n c \gamma} \quad (2.25)$$

The radar constant, k_c , will be input to the model. The variable σ will be determined by target of interest set during the simulation. Equation (2.24) provides radar detection range due to mainbeam clutter in terms of the two unknowns, R_c and ψ .

2.3.3 Detectability Factor. The required signal-to-noise ratio for target detection is the detectability factor and is represented by $D_x(n)$ where x represents the type of signal fluctuation modeled and n represents the number of pulses being integrated. Swerling designated targets with slow fluctuations in the radar cross section between pulses as Case 1 targets (6:81). Case 1 targets are assumed in this thesis effort. The signal-to-noise ratio is equal to the detectability factor for a steady target with one pulse integration, $D_0(1)$. Radars capable of integrating multiple pulses, reduce the required signal-to-noise ratio for detection. The detectability factor based on n pulses and a Case 1 Swerling model (6:71) is calculated by

$$D_1(n) = \frac{D_0(1)L_i(n)L_f(n)}{n} \quad (2.26)$$

where $D_0(1)$ is the detectability factor for Swerling Case 0, a steady target, and single pulse integration, $L_i(n)$ is the integration loss for n pulses in ratio form, $L_f(N)$ is the target fluctuation loss, and $D_1(n)$ is the n -pulse detectability factor for a Case 1 Swerling target. The equation for the detectability factor be rewritten as

$$D_1(n) = S/N \times I_n \quad (2.27)$$

where the integration factor, I_n , is given by

$$I_n = \frac{L_i(n)L_f(n)}{n} \quad (2.28)$$

2.4 TAC BRAWLER Air Combat Model

TAC BRAWLER is a multiple aircraft air combat computer simulation. It models the many complex aspects of aircraft and pilot performance to provide results of multiple aircraft air combat. TAC BRAWLER is used by AFCSA/SAGF to evaluate weapon system performance for various combat scenarios. For each aircraft participating in the simulation, TAC BRAWLER requires data to model the aircraft's performance, radar cross section, engine exhaust temperature, weapon configuration, and radar capabilities. Important to this thesis are the methods used to model radar performance. Data for most of the US fighter aircraft are available, but the data is classified. However, data is also available for an unclassified aircraft system. This thesis will use the unclassified data base to develop a methodology for determining radar detection range. This methodology can then be applied to the classified systems.

2.4.1 TAC BRAWLER's Radar Model. The radar model used in TAC BRAWLER has been validated with test data and evaluation (7:4.2-2). The radar detection range model is an iterative type model. The simulation determines whether target aircraft are in the search volume of the radar for each frame event. A frame event is considered one pass of the radar through its search volume. After each frame event, for targets within the search volume of the radar, TAC BRAWLER computes a total signal-to-noise ratio, S_n , as defined by (7:E-2)

$$S_n = \frac{S}{N + C} \quad (2.29)$$

which can be rewritten as

$$S_n = [(S/N)^{-1} + (S/C)^{-1}]^{-1} \quad (2.30)$$

The equation used in TAC BRAWLER for S/N is given by

$$S/N = \frac{P_{avg} G_{mb}^2 \sigma L_{mb} \lambda^2}{(4\pi)^3 F_n k T_o B_f R^4} \quad (2.31)$$

where G_{mb} is the mainbeam gain, and L_{mb} is the mainbeam loss. The only differences between this equation and equation (2.13) developed from Barton are because TAC BRAWLER assumes G_t and G_r are equal and the losses, L_t and L_α , the propagation factor, F , and the integration factor I_n are combined into one factor L_{mb} . The equation used for S/C is identical to the equation developed from Barton. On each frame event, TAC BRAWLER determines the probability of detection associated with the calculated S_n using a cumulative distribution function. A random number is generated to determine if radar detection occurs. For example, if the value of S_n is low, the probability of detection will be low. The draw for a random number should have a low probability of producing a radar detection.

2.4.2 Using TAC BRAWLER to Determine Radar Detection Range. Scenarios can easily be constructed for a 1 v 1 intercept. The 1 v 1 represents one attacker against one target. A flight scenario is constructed for each aircraft to participate in the simulation. Each aircraft is given a starting point in x, y coordinates, an altitude, a speed, and a position to fly to. The attacker's radar parameters must be specified, as well as the radar cross section of the target. With the proper initial conditions the aircraft will begin the intercept outside detection range and fly toward each other maintaining the proper altitude

and speed. By properly centering the search volume in the radar parameter data base, the target will always be evaluated for radar detection. At radar detection the simulation can be terminated and the radar detection range recorded.

2.5 Summary

The radar range equations developed from Barton identify the important parameters for determining radar detection range: the target's radar cross section, the ground reflectivity, range to the target, range to the clutter, the grazing angle, and the radar's parameters. Additionally, radar detection range with clutter as the source of interference is dependent on the relative velocities of the aircraft. The radar range equations can be used to determine radar detection range for a given detectability factor value. TAC BRAWLER incorporates an iterative radar detection range model to determine radar detection range. TAC BRAWLER can be used as a source for data to support this thesis.

III. METHODOLOGY

3.1 Overview

Research initially concentrated on the development of a closed form equation to determine radar detection range with clutter as the dominant source of interference. An equation which could provide a direct solution for radar detection range would be ideal. For several reasons this effort failed to provide a solution to the research objective. A short summary is provided to describe the methodology used in efforts to develop the closed form equations. However, the research objective was achieved using response surface methodology (RSM) and data from TAC BRAWLER. As a result, more detail is provided on the methodology for using RSM, the process of selecting the *best* regression equation, and incorporation of the regression equation into air combat simulations.

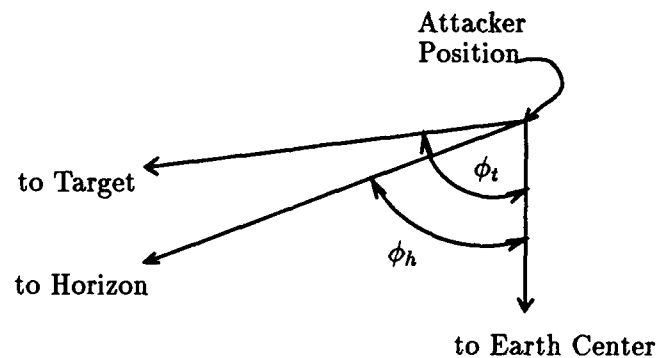


Figure 3.1. Angles of Incidence

3.2 Closed Form Equations

The radar detection range based on noise as the dominant source of interference, $R_{s/n}$, is easily calculated using equation (2.14). By determining $R_{s/n}$, the angle of incidence to

the target, ϕ_t , can be compared to the angle of incidence to the horizon, ϕ_h . Angle of incidence is the angle formed by two vectors originating at the attacker's position, with one pointed straight down and the other toward the object of interest (i.e. the horizon or the target). Figure 3.1 illustrates the angles of incidence for a target above the horizon. The equations required to make this comparison are

$$\phi_t = \arccos \left(\frac{R_{s/n}^2 + (R_e + A_h)^2 - (R_e + T_h)^2}{2R_{s/n}(R_e + A_h)} \right) \quad (3.1)$$

$$\phi_h = \arcsin \left(\frac{R_e}{(R_e + A_h)} \right) \quad (3.2)$$

where R_e is the effective radius of the earth in meters and A_h and T_h are the altitudes, height, of the attacker and target in meters, respectively. Figure 3.2 shows the geometry for determining ϕ_t . Similarly, Figure 3.3 shows the geometry for determining ϕ_h . The

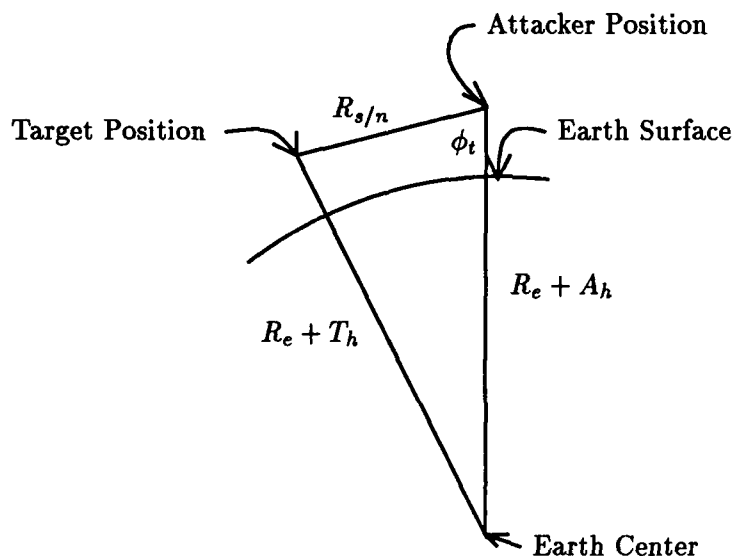


Figure 3.2. Attacker and Target Geometry

effective radius of the earth is 4/3 the physical radius (4:62). The increase is because the radar beam is deflected toward the earth by the atmosphere, which allows the radar beam

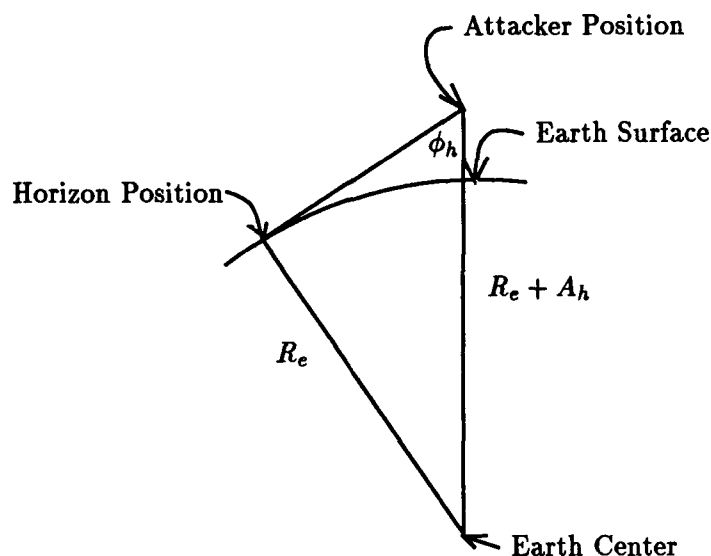


Figure 3.3. Attacker and Horizon Geometry

to be modelled as a straight line. If ϕ_t is greater than ϕ_h , the target is detected above the horizon and the detection range is $R_{s/n}$. If ϕ_h is greater than ϕ_t , the target is below the horizon and detection range must also be calculated based on clutter as the dominant source of interference. Radar detection range would be limited to the minimum value of $R_{s/n}$ and $R_{s/c}$. However, the calculation of $R_{s/c}$ involves three unknowns.

The geometry of the intercept can be used to establish two additional relationships for the three variables in the detection range equation based on clutter. The range equation is

$$R_{s/c} = \frac{k_c \sigma R_c^3}{\tan \psi} \quad (3.3)$$

where the three unknown variables are $R_{s/c}$, R_c , and ψ . Appendix A provides equations to solve for $R_{s/c}$ and ψ in terms of R_c . The equation resulting from these substitutions contains only one variable, R_c ; however, the equation is irreducible. A univariate search can be used to determine the value of R_c which satisfies the equation. Unfortunately, it

takes as many as 8 iterations to produce a solution with a resolution less than 1 nautical mile. Because investigations for a closed form equation led to the necessity of a univariate search, and numerous calculations to determine if noise or clutter is the dominant source of interference, the closed form equation approach was abandoned. However, significant insight into the problem was achieved and the progress developed for a closed form equation may be useful for future research.

3.3 *Response Surface Methodology*

Response surface methodology (RSM) uses statistical techniques to design and analyse experiments relating a *response* to a linear combination of *predictors* (8:1). One of the major applications of RSM is to estimate a response variable within limited regions of the predictor values (8:17). The contour generated by the response values mapped over specified ranges of predictor values forms the *response surface*. A response surface relating radar detection range to a set of target and/or attacker parameters would be ideal for satisfying the research objective.

Several considerations must be made to properly employ RSM to obtain a polynomial for estimating radar detection range. First, the variables to use as predictors must be determined. Second, the number of levels at which the variables will be input into TAC BRAWLER must be determined with appropriate bounds on the predictors. Third, the experimental design, *i.e.* the combinations of predictor levels, and the number of replications must be minimized to limit the required computer time for running TAC BRAWLER. Each of these considerations is discussed individually.

3.3.1 Predictors. The following variables will be used as predictors: target radar cross section, target altitude, attacker altitude, and the sum of the target and attacker velocities. The target's radar cross section is selected since it is included in the radar range equations. The altitudes are included because they define the relationships between range and grazing angle used in the clutter range equation. The decision to create one predictor with the sum of the aircraft airspeeds is partially motivated to reduce the number of predictors. Additional support for summing the airspeeds is because airspeed is the magnitude of the aircraft's velocity vector which determines the closing velocity between the aircraft. The term *airspeed sum* is used to refer to the sum of the aircraft airspeeds.

3.3.2 Predictor Levels. Due to the powers of 3 and 4 which are present in the range equations (2.14 and 2.24) a three level design was selected. A three level design is required for nonlinear response surfaces and radar detection range should be very nonlinear. Table 1 presents the values of the predictors at the three levels.

LEVEL	TARGET RCS (m^2)	TARGET ALTITUDE (ft)	ATTACKER ALTITUDE (ft)	AIRSPEED SUM (Mach)
-1	1	200	25000	1.256
0	5.5	600	17500	1.402
1	10	1000	10000	1.548

Table 3.1. Predictor Values and Levels

3.3.3 Experimental Design and Replications. The suggested experimental design for four predictors and three levels is a 3^4 design, which is read-three to the fourth. There

TARGET RCS	TARGET ALTITUDE	ATTACKER ALTITUDE	AIRSPEED SUM
± 1	± 1	0	0
0	0	± 1	± 1
0	0	0	0
± 1	0	0	± 1
0	± 1	± 1	0
0	0	0	0
± 1	0	± 1	0
0	± 1	0	± 1
0	0	0	0

Table 3.2. Fractional Design for Experimental Runs

are 81 possible combinations of the predictor levels. Due to the computer time required for running TAC BRAWLER a reduction in the number of combinations is desired. Box and Behnken developed experimental designs which use only a fraction of the possible combinations. For a 3^4 design, Box and Behnken (9:458) recommend the fractional design presented in Figure 3.2. Data was collected for ten replications of the design points listed in Table 3.2. Actually, there were 30 repetitions at the center point (0,0,0,0). There is no apriori method to determine the number of replications required. Regression analysis will indicate if additional repetitions are required to obtain a better model.

3.4 *Selecting the Best Regression Equation.*

The predictors, cross-products, and squared values will be used as variables for inclusion in the regression analysis. The inclusion of cross-product and squared variables assumes there will be nonlinear effects in the regression equation. Their inclusion bypasses

a step usually taken to regress only the predictors and then test for a lack of fit due to nonlinearity. If the effects are truly linear the cross-product and squared values will be left out of the regression equation due to their insignificance. The cost of including too many variables is computer time for the SAS runs which is insignificant for this application.

There is no unique statistical procedure for selecting the *best* regression equation. Draper and Smith identified ten different procedures commonly used for regression analysis which do not necessarily lead to the same solution for an identical problem (10:294,295). The difficulty lies in the balance between too few and too many variables. Too few variables do not explain the variance in the data and too many variables may explain the variance in the data at the expense of predictive power. The loss in predictive power is due to the regression equation being tailored specifically for the sample data. The resulting regression equation may match the sample data points very well, but produce large errors at intermediate points. The procedure used in this thesis to select the best regression equation will be the Mallows C_p statistic. The procedure uses

$$C_p = RSS_p / s^2 - (n - 2p) \quad (3.4)$$

where RSS_p is the residual sum of squares, p is the number of variables in the regression plus one, n is the number of data points collected, and s^2 is the residual mean square from the regression using all the variables(10:300). This procedure is stepwise in that the best regression equation for one variable is determined, then for two, three, and eventually all variables. The best regression equation for a particular number of variables is based on maximizing R^2 . A stepwise regression option, maxr, is available in SAS to automatically

determine the regression equation with the highest R^2 value and the associated C_p statistic for each possible setting of p . According to Draper and Smith, regression equations with C_p values less than or approximately equal to p will not suffer from a lack of fit. Regression equations that have C_p values far less than p may use more variables than required to fit the data, thus losing predictive power as described above. Once a regression equation is selected, the residuals will be evaluated to ensure they are normally distributed and are not biased by the value of the prediction.

The regression equation can be validated using additional TAC BRAWLER data at test points not identified in the experimental design matrix. The six test points are listed in Table 3.3 which identifies both the variable level and value. The detection range calculated

TEST POINT	TARGET RCS (m^2/lvl)	TARGET ALTITUDE (ft/lvl)	ATTACKER ALTITUDE (ft/lvl)	AIRSPEED SUM (Mach/lvl)
1	2/-.7777	500/-.25	15000/-.3333	1.35/-.3562
2	2/-.7777	500/-.25	20000/0.3333	1.5/0.6712
3	3/-.5555	700/.25	11000/-.8666	1.3/-.6986
4	3/-.5555	700/.25	20000/0.3333	1.3/-.6986
5	7/.3333	300/-.75	12000/-.7333	1.45/-.3288
6	7/.3333	600/0.00	19000/0.2	1.35/-.3562

Table 3.3. Test Point Values and Levels

by the regression equation can be evaluated against the 95% confidence intervals for the test points. This evaluation will be the criteria for determining successful accomplishment of the research objective.

3.5 Incorporating the Solution

Air combat simulations should be able to easily adopt the regression equation for determining radar detection range. The simulation will be required to keep track of the variables identified in the regression equation. The only complication is the requirement to convert the raw values of the variables to levels. Conversions are accomplished using

$$\text{variable level} = \frac{\text{variable value} - \text{midpoint value}}{.5 \times \text{value range}} \quad (3.5)$$

For RCS, the conversion is

$$\text{RCS level} = \frac{\text{RCS value} - 5.5}{4.5} \quad (3.6)$$

Additionally, each radar included in the simulation will require input data for the coefficients of the variables and the intercept value. Predetermined detection ranges can then be calculated using the variables, their coefficients, and the intercept.

IV. RESULTS

This chapter provides results from accomplishing the methodology previously described. Conclusions will be presented in Chapter V. Whenever possible results are reported in tables and the text of this chapter. Additional results are also provided in appendices.

4.1 TAC BRAWLER Results

Detection range data from TAC BRAWLER is provided in Appendix B for the 270 runs used in the regression analysis. Data for each run includes: the observation number, the target's radar cross section, the target's altitude, the attacker's altitude, the sum of the aircraft velocities, and the detection range in nautical miles. Detection range data from TAC BRAWLER for the test data points is presented in Appendix C.

p	C_p	R^2
4	16.25	.869
5	13.08	.871
6	10.29	.873
7	7.11	.876
8	5.93	.878
9	5.24	.879
10	5.99	.880

Table 4.1. Mallows C_p Statistic Summary

4.2 Regression Results

Appendix D provides a copy of the SAS file and output for the regression analysis. Table 4.1 provides the values for p , C_p , R^2 , for each regression equation. Based on Mallows C_p statistic the best regression equation results when p is 7 and the included variables are: RCS, attacker altitude, airspeed sum, RCS squared, target altitude squared, and attacker altitude squared. The regression equation for predicting radar detection range with these variables is

$$\begin{aligned} \text{Detection Range} = & 96.161 + 37.028(RCS) + 6.570(\text{Attacker Altitude}) - \\ & 2.098(\text{Airspeed Sum}) - 15.615(RCS)^2 + \\ & 3.451(\text{Target Altitude})^2 + 3.034(\text{Attacker Altitude})^2 \quad (4.1) \end{aligned}$$

This equation has an R^2 value of .876 meaning 87.6% of the variance in the data is explained by the regression. A separate regression run was accomplished for these variables to evaluate two plots. The first plotted the residuals vs the predicted value to ensure a transformation of the observed detection ranges was not required. The second plotted the residuals vs the residual's rank to ensure the residuals were normally distributed. Appendix C contains both of these plots which indicate no transformation is required and the residuals are normally distributed.

Results from the test points are presented in Table 4.2. The predicted values for five of the test points are well within the 95% confidence interval of the sample data. Test point 6 lies just outside the confidence interval. In absolute numbers the predicted value is 109.0 nautical miles (nm) compared to a sample mean of 101.3 nm. The difference is

TEST POINT	PREDICTED VALUE	SAMPLE MEAN	PREDICTION MINUS MEAN	SAMPLE STANDARD DEVIATION	CONFIDENCE INTERVAL
1	57.0	58.1	-1.1	9.4	51.4 - 64.8
2	59.2	66.0	-6.8	11.6	57.7 - 74.3
3	69.0	73.8	-4.8	7.0	68.8 - 78.8
4	75.0	72.9	2.1	6.8	68.0 - 77.8
5	104.8	104.8	0.0	6.7	100.0 - 109.6
6	109.0	101.3	7.7	8.9	94.9 - 107.7

Table 4.2. Validation Results

less than 8 nm at a range over 100 nm. The detection range data for test point 6 includes one observation that is almost 2 standard deviations from the mean.

V. CONCLUSIONS AND RECOMMENDATIONS

5.1 Conclusions

The best regression equation for predicting radar detection range is

$$\begin{aligned} \text{Detection Range} = & 96.161 + 37.028(RCS) + 6.570(\text{Attacker Altitude}) - \\ & 2.098(\text{Airspeed Sum}) - 15.615(RCS)^2 + \\ & 3.451(\text{Target Altitude})^2 + 3.034(\text{Attacker Altitude})^2 \quad (5.1) \end{aligned}$$

This equation appropriately fits the data based on Mallows C_p statistic. The equation also makes sense. The most significant variable in the range equations is the target's RCS. The two variables with the the largest coefficients in the regression equation are RCS and RCS^2 . Of the other two main effects, attacker altitude has the next largest coefficient. This makes sense because for a fixed point target surface clutter is reduced as attacker altitude decreases since range to the surface clutter increases. The negative coefficient for airspeed sum was less intuitive to explain. However, as closure rates increase the target travels further between radar scans and is able to penetrate further before detection. The inclusion of the squared values of attacker and target altitudes are indicative of the nonlinear relationship expected for the effect of grazing angle on the surface clutter return. The residual plots indicate the residuals are not correlated with the predicted value and are normally distributed. If either of these conditions existed the regression equation could have been improved. The regression equation explains 87.6% of the variation in the data

generated by TAC BRAWLER. For the purpose of this thesis 87.6% is acceptable, a higher R^2 could possibly be achieved by including more repetitions in the regression.

Predictions for the test points using equation (5.1) support acceptance of the regression equation also. Five of the detection ranges lie well within the confidence intervals. The sixth test point lies just outside the confidence interval. TAC BRAWLER data for this point includes one observation that is significantly below the others. The failure of the sixth data point is attributed to the small sample size. In terms of absolute differences, three of the test points were within 2.1 nm and all were within 7.7 nm of the sample data. As a result, the test points validate the performance of the regression equation to predict radar detection range.

Equation (5.1) can be easily incorporated in air combat simulations to model radar performance and provide predetermined detection ranges. The regression equation serves as a meta-model of TAC BRAWLER's detection range model.

5.2 Recommendations

5.2.1 Applications. The complexity of the parent air combat simulation drives the requirements for the radar model. Multiple response surfaces could be used if the bounds on the variables need to be expanded. For example, a supplemental response surface could be generated for targets with altitudes between 1000 and 5000 feet. Radar detection range could then be calculated using the appropriate equation for the target's altitude. The methodology for determining each additional regression equation would be the same. If

necessary, variance reduction could be accomplished using additional repetitions at the experimental design points.

5.2.2 Future Research. The development of a closed form equation for calculating radar detection range in clutter would be significant. A closed form equation would eliminate the data collection efforts required to develop response surfaces. Analysis in this thesis was limited to comparisons between the predictions and TAC BRAWLER data. An addition step to compare the predictions with actual aircraft data is recommended.

Appendix A. CLOSED FORM SOLUTION

A.1 Intercept Geometry

The geometry between the attacker and the target can be used to establish two additional relationships between the unknown variables: R , R_c , and ψ . Figure A.1 illustrates the intercept geometry.

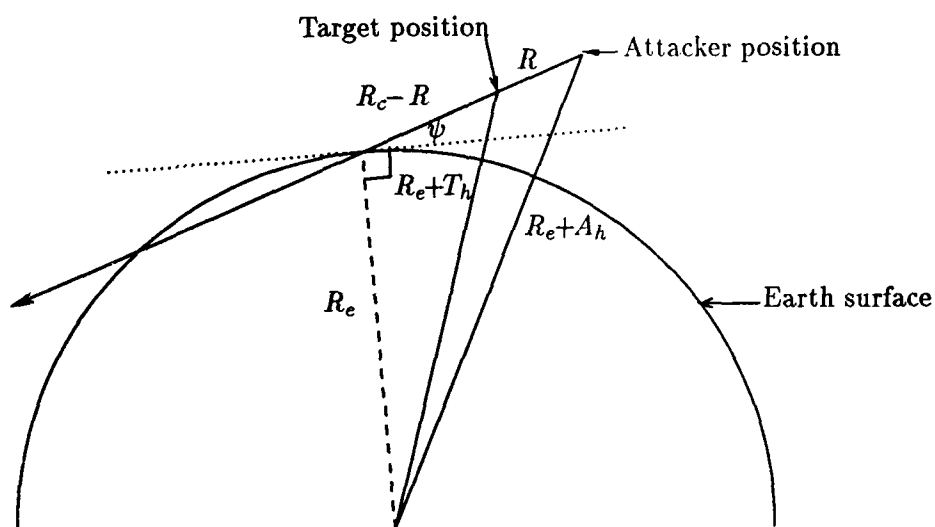


Figure A.1. Intercept Geometry

The law of cosines establishes the following equations:

$$(R_e + A_h)^2 = R_e^2 + R_c^2 - 2R_e R_c \cos(90 + \psi) \quad (\text{A.1})$$

$$(R_e + T_h)^2 = R_e^2 + (R_c - R)^2 - 2R_e (R_c - R) \cos(90 + \psi) \quad (\text{A.2})$$

Setting the left hand side of equations (A.1 and A.2) equal to zero and using the quadratic equation provides solutions for R_c and $R_c - R$ in terms of ψ . The following equations show the solution steps.

$$0 = R_c^2 - 2R_e \cos(90 + \psi)R_c + R_e^2 - (R_e + A_h)^2 \quad (\text{A.3})$$

$$0 = (R_c - R)^2 - 2R_e \cos(90 + \psi)(R_c - R) + R_e^2 - (R_e + T_h)^2 \quad (\text{A.4})$$

$$R_c = 2R_e \cos(90 + \psi) (2^{-1}) \pm (2^{-1}) \sqrt{(-2R_e \cos(90 + \psi))^2 - 4(R_e^2 - (R_e + A_h)^2)} \quad (\text{A.5})$$

$$R_c - R = 2R_e \cos(90 + \psi) (2^{-1}) \pm (2^{-1}) \sqrt{(-2R_e \cos(90 + \psi))^2 - 4(R_e^2 - (R_e + T_h)^2)} \quad (\text{A.6})$$

$$R_c = R_e \cos(90 + \psi) \pm \sqrt{R_e^2 \cos^2(90 + \psi) - R_e^2 + (R_e + A_h)^2} \quad (\text{A.7})$$

$$R_c - R = R_e \cos(90 + \psi) \pm \sqrt{R_e^2 \cos^2(90 + \psi) - R_e^2 + (R_e + T_h)^2} \quad (\text{A.8})$$

$$R_c = R_e \cos(90 + \psi) \pm \sqrt{R_e^2(1 - \sin^2(90 + \psi)) - R_e^2 + (R_e + A_h)^2} \quad (\text{A.9})$$

$$R_c - R = R_e \cos(90 + \psi) \pm \sqrt{R_e^2(1 - \sin^2(90 + \psi)) - R_e^2 + (R_e + T_h)^2} \quad (\text{A.10})$$

$$R_c = R_e \cos(90 + \psi) \pm \sqrt{(R_e + A_h)^2 - R_e^2 \sin^2(90 + \psi)} \quad (\text{A.11})$$

$$R_c - R = R_e \cos(90 + \psi) \pm \sqrt{(R_e + T_h)^2 - R_e^2 \sin^2(90 + \psi)} \quad (\text{A.12})$$

The positive values from the square roots provide the ranges of interest. Therefore, the equations for R_c and $R_c - R$ are

$$R_c = R_e \cos(90 + \psi) + \sqrt{(R_e + A_h)^2 - R_e^2 \sin^2(90 + \psi)} \quad (\text{A.13})$$

$$R_c - R = R_e \cos(90 + \psi) + \sqrt{(R_e + T_h)^2 - R_e^2 \sin^2(90 + \psi)} \quad (\text{A.14})$$

Equations (2.24, A.13, and A.14) can be solved simultaneously to determine radar detection range based on clutter as the dominant source of interference.

A.2 Solving for $\tan \psi$ in Terms of R_c

Equation (A.13) can be rewritten and manipulated to solve for $\tan \psi$ in terms of R_c .

$$R_c - R_e \cos(90 + \psi) = \sqrt{(R_e + A_h)^2 - R_e^2 \sin^2(90 + \psi)} \quad (\text{A.15})$$

$$\begin{aligned} R_c^2 - 2R_c R_e \cos(90 + \psi) &= (R_e + A_h)^2 - R_e^2 \sin^2(90 + \psi) - \\ &\quad R_e^2 \cos^2(90 + \psi) \end{aligned} \quad (\text{A.16})$$

$$\begin{aligned} R_c^2 - 2R_c R_e \cos(90 + \psi) &= (R_e + A_h)^2 - \\ &\quad R_e^2(\sin^2(90 + \psi) + \cos^2(90 + \psi)) \end{aligned} \quad (\text{A.17})$$

$$R_c^2 - 2R_c R_e \cos(90 + \psi) = (R_e + A_h)^2 - R_e^2(1) \quad (\text{A.18})$$

$$-2R_c R_e \cos(90 + \psi) = -R_c^2 + (R_e + A_h)^2 - R_e^2 \quad (\text{A.19})$$

$$-2R_c R_e \cos(90 + \psi) = -R_c^2 + R_e^2 + 2R_e A_h + A_h^2 - R_e^2 \quad (\text{A.20})$$

$$-2R_c R_e \cos(90 + \psi) = -R_c^2 + 2R_e A_h + A_h^2 \quad (\text{A.21})$$

A useful substitution for $2R_e A_h + A_h^2$ is k_a . The derivation continues with

$$-2R_c R_e \cos(90 + \psi) = k_a - R_c^2 \quad (\text{A.22})$$

$$\cos(90 + \psi) = \frac{R_c^2 - k_a}{2R_c R_e} \quad (\text{A.23})$$

$$-\sin(\psi) = \frac{R_c^2 - k_a}{2R_c R_e} \quad (\text{A.24})$$

$$\sin(\psi) = \frac{k_a - R_c^2}{2R_c R_e} \quad (\text{A.25})$$

$$\tan(\psi) = \frac{(k_a - R_c^2)/(2R_c R_e)}{\sqrt{1 - [(k_a - R_c^2)/(2R_c R_e)]^2}} \quad (\text{A.26})$$

A.3 Solving for R in Terms of R_c

Equation (A.14) can be subtracted from equation (A.13) and written as

$$R = \sqrt{(R_e + A_h)^2 - R_e^2 \sin^2(90 + \psi)} - \sqrt{(R_e + T_h)^2 - R_e^2 \sin^2(90 + \psi)} \quad (\text{A.27})$$

Using the identity $\sin^2(90 + \psi) = 1 - \sin^2(\psi)$ the equation can be rewritten as

$$R = \sqrt{(R_e + A_h)^2 - R_e^2(1 - \sin^2(\psi))} - \sqrt{(R_e + T_h)^2 - R_e^2(1 - \sin^2(\psi))} \quad (\text{A.28})$$

$$R = \sqrt{R_e^2 + 2R_e A_h + A_h^2 - R_e^2 + R_e^2 \sin^2(\psi)} - \sqrt{R_e^2 + 2R_e A_h + T_h^2 - R_e^2 + R_e^2 \sin^2(\psi)} \quad (\text{A.29})$$

$$R = \sqrt{2R_e A_h + A_h^2 + R_e^2 \sin^2(\psi)} - \sqrt{2R_e A_h + T_h^2 + R_e^2 \sin^2(\psi)} \quad (\text{A.30})$$

Substituting for $\sin \psi$, putting in k_a and a similar term, k_t for $2R_e T_h + T_h^2$, results in

$$R = \sqrt{k_a + R_c^2(k_a - R_c^2)^2/4R_c^2R_c^2} - \sqrt{k_t + R_c^2(k_a - R_c^2)^2/4R_c^2R_c^2} \quad (\text{A.31})$$

$$R = \sqrt{k_a + (k_a - R_c^2)^2/4R_c^2} - \sqrt{k_t + (k_a - R_c^2)^2/4R_c^2} \quad (\text{A.32})$$

$$R = \left(\sqrt{4k_aR_c^2 + k_a^2 - 2k_aR_c^2 + R_c^4} - \sqrt{4k_tR_c^2 + k_a^2 - 2k_aR_c^2 + R_c^4} \right) / 2R_c \quad (\text{A.33})$$

$$R = \left(\sqrt{k_a^2 + 2k_aR_c^2 + R_c^4} - \sqrt{k_a^2 + (4k_t - 2k_a)R_c^2 + R_c^4} \right) / 2R_c \quad (\text{A.34})$$

$$R = \left(k_a + R_c^2 - \sqrt{k_a^2 + (4k_t - 2k_a)R_c^2 + R_c^4} \right) / 2R_c \quad (\text{A.35})$$

A.4 Single Variable Range Equation

The maximum detection range for clutter interference is given by

$$R_{s/c}^4 = \frac{k_c \sigma R_c^3}{\tan \psi} \quad (\text{A.36})$$

where R is equal to $R_{s/c}$ based on the minimum value of the detectability factor used in k_c .

Substituting for $R_{s/c}$ and $\tan \psi$ results in

$$\left[(k_a + R_c^2 - \sqrt{k_a^2 + (4k_t - 2k_a)R_c^2 + R_c^4}) / 2R_c \right]^4 = k_c \sigma R_c^3 \left(\frac{\sqrt{1 - (k_a - R_c^2)^2 / (4R_c^2R_c^2)}}{(k_a - R_c^2) / (2R_cR_e)} \right) \quad (\text{A.37})$$

Although equation (A.37) has only one unknown, the form is not acceptable for a predetermined detection range model. The numerous calculations required defeat the objective of this thesis. As a result, another methodology was adopted.

Appendix B. TAC BRAWLER ~~Data~~ DATA

The following detection range data was generated using TAC BRAWLER.

OBSERVATION	TARGET RCS	TARGET ALTITUDE	ATTACKER ALTITUDE	VELOCITY SUM	DETECTION RANGE
1	1	1	0	0	104.6127
2	1	1	0	0	143.9742
3	1	1	0	0	126.6151
4	1	1	0	0	117.0360
5	1	1	0	0	101.5475
6	1	1	0	0	121.3766
7	1	1	0	0	116.1495
8	1	1	0	0	94.4717
9	1	1	0	0	111.1776
10	1	1	0	0	129.6794
11	1	-1	0	0	116.4361
12	1	-1	0	0	139.4184
13	1	-1	0	0	131.0922
14	1	-1	0	0	130.8570
15	1	-1	0	0	125.4423
16	1	-1	0	0	113.2288
17	1	-1	0	0	121.5940
18	1	-1	0	0	135.0567
19	1	-1	0	0	98.4325
20	1	-1	0	0	112.8514
21	-1	1	0	0	37.3875
22	-1	1	0	0	46.4316
23	-1	1	0	0	52.5769
24	-1	1	0	0	48.3503
25	-1	1	0	0	48.5717
26	-1	1	0	0	52.8305
27	-1	1	0	0	45.4480
28	-1	1	0	0	53.0602
29	-1	1	0	0	47.4530
30	-1	1	0	0	39.9885

OBSERVATION	TARGET RCS	TARGET ALTITUDE	ATTACKER ALTITUDE	VELOCITY SUM	DETECTION RANGE
31	-1	-1	0	0	43.2786
32	-1	-1	0	0	39.0955
33	-1	-1	0	0	46.8768
34	-1	-1	0	0	50.8252
35	-1	-1	0	0	40.0127
36	-1	-1	0	0	43.1030
37	-1	-1	0	0	42.7138
38	-1	-1	0	0	44.5660
39	-1	-1	0	0	53.2149
40	-1	-1	0	0	54.6048
41	0	0	1	1	120.9492
42	0	0	1	1	81.7799
43	0	0	1	1	112.4125
44	0	0	1	1	96.7358
45	0	0	1	1	97.5982
46	0	0	1	1	91.0797
47	0	0	1	1	107.3052
48	0	0	1	1	106.8166
49	0	0	1	1	96.0532
50	0	0	1	1	98.5373
51	0	0	1	-1	123.5864
52	0	0	1	-1	114.7908
53	0	0	1	-1	114.9478
54	0	0	1	-1	97.6185
55	0	0	1	-1	108.6818
56	0	0	1	-1	113.0049
57	0	0	1	-1	93.8200
58	0	0	1	-1	97.4075
59	0	0	1	-1	103.7933
60	0	0	1	-1	122.5736
61	0	0	-1	1	99.6171
62	0	0	-1	1	91.6354
63	0	0	-1	1	102.4275
64	0	0	-1	1	88.4687
65	0	0	-1	1	108.8589
66	0	0	-1	1	98.6036
67	0	0	-1	1	101.2283
68	0	0	-1	1	87.3331
69	0	0	-1	1	88.0013
70	0	0	-1	1	95.5104

OBSERVATION	TARGET RCS	TARGET ALTITUDE	ATTACKER ALTITUDE	VELOCITY SUM	DETECTION RANGE
71	0	0	-1	-1	98.5180
72	0	0	-1	-1	81.5019
73	0	0	-1	-1	101.7528
74	0	0	-1	-1	89.0612
75	0	0	-1	-1	88.5676
76	0	0	-1	-1	106.3737
77	0	0	-1	-1	88.6160
78	0	0	-1	-1	91.6233
79	0	0	-1	-1	98.4081
80	0	0	-1	-1	84.2132
81	0	0	0	0	85.7069
82	0	0	0	0	85.4200
83	0	0	0	0	80.8230
84	0	0	0	0	93.4011
85	0	0	0	0	71.9412
86	0	0	0	0	103.4311
87	0	0	0	0	78.8588
88	0	0	0	0	94.3215
89	0	0	0	0	101.8817
90	0	0	0	0	93.0346
91	1	0	0	1	119.7691
92	1	0	0	1	121.8145
93	1	0	0	1	105.3479
94	1	0	0	1	103.7536
95	1	0	0	1	120.5390
96	1	0	0	1	109.9275
97	1	0	0	1	115.2997
98	1	0	0	1	115.7075
99	1	0	0	1	136.1237
100	1	0	0	1	124.8521
101	1	0	0	-1	123.4037
102	1	0	0	-1	144.8449
103	1	0	0	-1	132.1935
104	1	0	0	-1	128.6728
105	1	0	0	-1	134.1219
106	1	0	0	-1	120.5336
107	1	0	0	-1	127.2152
108	1	0	0	-1	112.8700
109	1	0	0	-1	125.2167
110	1	0	0	-1	112.4332

OBSERVATION	TARGET RCS	TARGET ALTITUDE	ATTACKER ALTITUDE	VELOCITY SUM	DETECTION RANGE
111	-1	0	0	1	49.9619
112	-1	0	0	1	33.8024
113	-1	0	0	1	29.3796
114	-1	0	0	1	55.3693
115	-1	0	0	1	23.0820
116	-1	0	0	1	33.6146
117	-1	0	0	1	43.0263
118	-1	0	0	1	25.1195
119	-1	0	0	1	50.3387
120	-1	0	0	1	39.8883
121	-1	0	0	-1	50.7589
122	-1	0	0	-1	63.6341
123	-1	0	0	-1	46.4654
124	-1	0	0	-1	36.5711
125	-1	0	0	-1	56.7504
126	-1	0	0	-1	37.8363
127	-1	0	0	-1	59.6368
128	-1	0	0	-1	48.2739
129	-1	0	0	-1	50.8489
130	-1	0	0	-1	39.8900
131	0	1	1	0	99.3465
132	0	1	1	0	121.6694
133	0	1	1	0	113.5586
134	0	1	1	0	103.5680
135	0	1	1	0	111.6760
136	0	1	1	0	98.3197
137	0	1	1	0	99.2522
138	0	1	1	0	99.2957
139	0	1	1	0	110.9767
140	0	1	1	0	120.3642
141	0	1	-1	0	89.3854
142	0	1	-1	0	98.2067
143	0	1	-1	0	103.4031
144	0	1	-1	0	97.9684
145	0	1	-1	0	97.4080
146	0	1	-1	0	99.6444
147	0	1	-1	0	92.4899
148	0	1	-1	0	90.7777
149	0	1	-1	0	116.4117
150	0	1	-1	0	105.5196

OBSERVATION	TARGET RCS	TARGET ALTITUDE	ATTACKER ALTITUDE	VELOCITY SUM	DETECTION RANGE
151	0	-1	1	0	106.8803
152	0	-1	1	0	109.9135
153	0	-1	1	0	116.2170
154	0	-1	1	0	119.8730
155	0	-1	1	0	98.2241
156	0	-1	1	0	99.0630
157	0	-1	1	0	94.3656
158	0	-1	1	0	118.5377
159	0	-1	1	0	113.0569
160	0	-1	1	0	111.1279
161	0	-1	-1	0	108.9813
162	0	-1	-1	0	91.2410
163	0	-1	-1	0	99.5271
164	0	-1	-1	0	97.9285
165	0	-1	-1	0	110.1265
166	0	-1	-1	0	102.6880
167	0	-1	-1	0	86.5833
168	0	-1	-1	0	98.7223
169	0	-1	-1	0	91.4285
170	0	-1	-1	0	88.7338
171	0	0	0	0	96.0587
172	0	0	0	0	119.1185
173	0	0	0	0	99.0687
174	0	0	0	0	96.1330
175	0	0	0	0	100.8157
176	0	0	0	0	95.9472
177	0	0	0	0	90.6688
178	0	0	0	0	90.5644
179	0	0	0	0	102.9638
180	0	0	0	0	92.6052
181	1	0	1	0	123.5327
182	1	0	1	0	119.5998
183	1	0	1	0	136.5825
184	1	0	1	0	113.4748
185	1	0	1	0	130.1631
186	1	0	1	0	132.5898
187	1	0	1	0	115.8202
188	1	0	1	0	122.7123
189	1	0	1	0	142.9473
190	1	0	1	0	125.1867

OBSERVATION	TARGET RCS	TARGET ALTITUDE	ATTACKER ALTITUDE	VELOCITY SUM	DETECTION RANGE
191	1	0	-1	0	96.7743
192	1	0	-1	0	95.4365
193	1	0	-1	0	102.0165
194	1	0	-1	0	134.2215
195	1	0	-1	0	115.4106
196	1	0	-1	0	106.8926
197	1	0	-1	0	101.1893
198	1	0	-1	0	116.9122
199	1	0	-1	0	111.7089
200	1	0	-1	0	115.2898
201	-1	0	1	0	51.3730
202	-1	0	1	0	38.5299
203	-1	0	1	0	53.9828
204	-1	0	1	0	40.7777
205	-1	0	1	0	56.7201
206	-1	0	1	0	64.3997
207	-1	0	1	0	67.7932
208	-1	0	1	0	69.9625
209	-1	0	1	0	61.7350
210	-1	0	1	0	69.9623
211	-1	0	-1	0	29.7531
212	-1	0	-1	0	51.9475
213	-1	0	-1	0	31.7333
214	-1	0	-1	0	37.1469
215	-1	0	-1	0	32.7561
216	-1	0	-1	0	28.4030
217	-1	0	-1	0	45.0819
218	-1	0	-1	0	32.0005
219	-1	0	-1	0	36.2939
220	-1	0	-1	0	35.7556
221	0	1	0	1	105.5049
222	0	1	0	1	98.2458
223	0	1	0	1	98.5533
224	0	1	0	1	97.4381
225	0	1	0	1	92.0718
226	0	1	0	1	111.1577
227	0	1	0	1	90.2007
228	0	1	0	1	98.3945
229	0	1	0	1	120.3328
230	0	1	0	1	92.3032

OBSERVATION	TARGET RCS	TARGET ALTITUDE	ATTACKER ALTITUDE	VELOCITY SUM	DETECTION RANGE
231	0	1	0	-1	86.2289
232	0	1	0	-1	103.5082
233	0	1	0	-1	119.7700
234	0	1	0	-1	109.6026
235	0	1	0	-1	88.8477
236	0	1	0	-1	92.4782
237	0	1	0	-1	103.3537
238	0	1	0	-1	102.7451
239	0	1	0	-1	112.9618
240	0	1	0	-1	102.3852
241	0	-1	0	1	92.6383
242	0	-1	0	1	89.1392
243	0	-1	0	1	105.7666
244	0	-1	0	1	106.7057
245	0	-1	0	1	101.8537
246	0	-1	0	1	101.3062
247	0	-1	0	1	100.4344
248	0	-1	0	1	119.2629
249	0	-1	0	1	82.4477
250	0	-1	0	1	90.2177
251	0	-1	0	-1	83.8898
252	0	-1	0	-1	79.4741
253	0	-1	0	-1	98.2684
254	0	-1	0	-1	109.1235
255	0	-1	0	-1	117.7504
256	0	-1	0	-1	111.1633
257	0	-1	0	-1	108.2004
258	0	-1	0	-1	81.1713
259	0	-1	0	-1	92.2830
260	0	-1	0	-1	99.1451
261	0	0	0	0	113.2521
262	0	0	0	0	94.9893
263	0	0	0	0	87.1786
264	0	0	0	0	81.5291
265	0	0	0	0	92.9966
266	0	0	0	0	109.2859
267	0	0	0	0	82.7539
268	0	0	0	0	104.2508
269	0	0	0	0	87.2543
270	0	0	0	0	98.1074

Appendix C. TEST POINT DATA

Results for each of the test points are presented below.

OBSERVATION	TEST POINT					
	1	2	3	4	5	6
1	50.9	80.0	76.9	73.3	95.5	98.0
2	65.3	51.2	68.0	66.6	106.5	107.5
3	65.3	63.8	81.6	71.8	109.6	100.4
4	49.8	73.6	64.2	63.0	110.4	113.3
5	45.8	62.1	76.3	83.3	106.1	93.8
6	68.8	70.8	64.2	70.9	94.3	103.3
7	66.6	43.0	81.9	80.4	108.6	106.5
8	67.8	66.1	67.9	64.6	114.6	111.4
9	47.2	77.0	78.4	75.6	96.0	93.5
10	53.6	72.5	78.6	79.1	106.6	85.2

Appendix D. SAS DATA

D.1 SAS MAXR Program File

```
options linesize=66;
data first;
infile tbi;
input RCS TGTALT ATKRALT VELSUM RNG;
RNG=RNG/6076.115;
RT=RCS*TGTALT;
RA=RCS*ATKRALT;
RV=RCS*VELSUM;
TA=TGTALT*ATKRALT;
TV=TGTALT*VELSUM;
AV=ATKRALT*VELSUM;
RSQ=RCS*RCS;
TSQ=TGTALT*TGTALT;
ASQ=ATKRALT*ATKRALT;
VSQ=VELSUM*VELSUM;
/*****Computer Selected Model*****/
proc stepwise;
    model RNG = RCS TGTALT ATKRALT VELSUM RT RA RV TA TV AV
            RSQ TSQ ASQ VSQ/stepwise maxr;
/*****Selected Model*****/
proc reg data = first;
model RNG = RCS ATKRALT VELSUM RSQ TSQ ASQ;
output out=a p=RNGhat r=rRNG;
    data residul;
        set a;
        error = rRNG/RNGhat;
        err = abs(error);
proc plot data = residul;
plot rRNG*RNGhat="R"/vref=0;
proc rank normal=vw;
    var rRNG;
    ranks rrRNG;
proc plot;
    plot rrRNG*rRNG;
```

D.2 SAS MAXR Output

MAXIMUM R-SQUARE IMPROVEMENT FOR DEPENDENT VARIABLE RNG

STEP 1 VARIABLE RCS ENTERED

R SQUARE = 0.75758298

C(P) = 249.82160935

	DF	SUM OF SQUARES	MEAN SQUARE	F	PROB>F
REGRESSION	1	164532.05721278	164532.0572	837.53	0.0001
ERROR	268	52648.18637075	196.4485		
TOTAL	269	217180.24358354			

	B VALUE	STD ERROR	TYPE II SS	F	PROB>F
INTERCEPT	92.10318021				
RCS	37.02837394	1.27948055	164532.0572	837.53	0.0001

THE ABOVE MODEL IS THE BEST 1 VARIABLE MODEL FOUND.

STEP 2 VARIABLE RSQ ENTERED

R SQUARE = 0.84538248

C(P) = 64.99942442

	DF	SUM OF SQUARES	MEAN SQUARE	F	PROB>F
REGRESSION	2	183600.37275463	91800.18638	729.92	0.0001
ERROR	267	33579.87082891	125.76731		
TOTAL	269	217180.24358354			

	B VALUE	STD ERROR	TYPE II SS	F	PROB>F
INTERCEPT	99.61974277				
RCS	37.02837394	1.02374845	164532.0572	1308.23	0.0001
RSQ	-16.91226576	1.37350267	19068.3155	151.62	0.0001

THE ABOVE MODEL IS THE BEST 2 VARIABLE MODEL FOUND.

STEP 3 VARIABLE ATKRALT ENTERED

R SQUARE = 0.86923291

C(P) = 16.24982448

	DF	SUM OF SQUARES	MEAN SQUARE	F	PROB>F
REGRESSION	3	188780.21467619	62926.73823	589.38	0.0001
ERROR	266	28400.02890735	106.76703		
TOTAL	269	217180.24358354			

	B VALUE	STD ERROR	TYPE II SS	F	PROB>F
INTERCEPT	99.61974277				
RCS	37.02837394	0.94325247	164532.0572	1541.04	0.0001
ATKRALT	6.57003420	0.94325247	5179.8419	48.52	0.0001
RSQ	-16.91226576	1.26550598	19068.3155	178.60	0.0001

THE ABOVE MODEL IS THE BEST 3 VARIABLE MODEL FOUND.

STEP 4 VARIABLE VELSUM ENTERED

R SQUARE = 0.87166453

C(P) = 13.07575323

	DF	SUM OF SQUARES	MEAN SQUARE	F	PROB>F
REGRESSION	4	189308.31482207	47327.07871	449.98	0.0001
ERROR	265	27871.92876146	105.17709		
TOTAL	269	217180.24358354			

	B VALUE	STD ERROR	TYPE II SS	F	PROB>F
INTERCEPT	99.61974277				
RCS	37.02837394	0.93620283	164532.0572	1564.33	0.0001
ATKRALT	6.57003420	0.93620283	5179.8419	49.25	0.0001
VELSUM	-2.09781661	0.93620283	528.1001	5.02	0.0259
RSQ	-16.91226576	1.25604791	19068.3155	181.30	0.0001

THE ABOVE MODEL IS THE BEST 4 VARIABLE MODEL FOUND.

STEP 5 VARIABLE ASQ ENTERED

R SQUARE = 0.87391335

C(P) = 10.29065239

	DF	SUM OF SQUARES	MEAN SQUARE	F	PROB>F
REGRESSION	5	189796.71406007	37959.34281	365.96	0.0001
ERROR	264	27383.52952347	103.72549		
TOTAL	269	217180.24358354			

	B VALUE	STD ERROR	TYPE II SS	F	PROB>F
INTERCEPT	96.16071868				
RCS	37.02837394	0.92971990	164532.0572	1586.23	0.0001
ATKRALT	6.57003420	0.92971990	5179.8419	49.94	0.0001
RSQ	-15.61513173	1.31482249	14629.9403	141.04	0.0001
TSQ	3.45148197	1.31482249	714.7637	6.89	0.0092
ASQ	3.03418819	1.31482249	552.3779	5.33	0.0218

THE ABOVE MODEL IS THE BEST 5 VARIABLE MODEL FOUND.

STEP 6 VARIABLE VELSUM ENTERED

R SQUARE = 0.87634497

C(P) = 7.11658115

	DF	SUM OF SQUARES	MEAN SQUARE	F	PROB>F
REGRESSION	6	190324.81420595	31720.80237	310.65	0.0001
ERROR	263	26855.42937759	102.11190		
TOTAL	269	217180.24358354			

	B VALUE	STD ERROR	TYPE II SS	F	PROB>F
INTERCEPT	96.16071868				
RCS	37.02837394	0.92246002	164532.0572	1611.29	0.0001
ATKRALT	6.57003420	0.92246002	5179.8419	50.73	0.0001
VELSUM	-2.09781661	0.92246002	528.1001	5.17	0.0238
RSQ	-15.61513173	1.30455547	14629.9403	143.27	0.0001
TSQ	3.45148197	1.30455547	714.7637	7.00	0.0086
ASQ	3.03418819	1.30455547	552.3779	5.41	0.0208

THE ABOVE MODEL IS THE BEST 6 VARIABLE MODEL FOUND.

STEP 7 VARIABLE AV ENTERED

R SQUARE = 0.87784110

C(P) = 5.93308329

	DF	SUM OF SQUARES	MEAN SQUARE	F	PROB>F
REGRESSION	7	190649.74318449	27235.67760	268.96	0.0001
ERROR	262	26530.50039905	101.26145		
TOTAL	269	217180.24358354			

	B VALUE	STD ERROR	TYPE II SS	F	PROB>F
INTERCEPT	96.16071868				
RCS	37.02837394	0.91861060	164532.0572	1624.82	0.0001
ATKRALT	6.57003420	0.91861060	5179.8419	51.15	0.0001
VELSUM	-2.09781661	0.91861060	528.1001	5.22	0.0232
AV	-2.85012710	1.59108023	324.9290	3.21	0.0744
RSQ	-15.61513173	1.29911157	14629.9403	144.48	0.0001
TSQ	3.45148197	1.29911157	714.7637	7.06	0.0084
ASQ	3.03418819	1.29911157	552.3779	5.45	0.0203

THE ABOVE MODEL IS THE BEST 7 VARIABLE MODEL FOUND.

STEP 8 VARIABLE VSQ ENTERED

R SQUARE = 0.87910342

C(P) = 5.24708502

	DF	SUM OF SQUARES	MEAN SQUARE	F	PROB>F
REGRESSION	8	190923.89404345	23865.48676	237.23	0.0001
ERROR	261	26256.34954008	100.59904		
TOTAL	269	217180.24358354			

	B VALUE	STD ERROR	TYPE II SS	F	PROB>F
INTERCEPT	94.14540377				
RCS	37.02837394	0.91560108	164532.0572	1635.52	0.0001
ATKRALT	6.57003420	0.91560108	5179.8419	51.49	0.0001
VELSUM	-2.09781661	0.91560108	528.1001	5.25	0.0227
AV	-2.85012710	1.58586759	324.9290	3.23	0.0735
RSQ	-14.85938863	1.37340162	11776.0763	117.06	0.0001
TSQ	4.20722507	1.37340162	944.0396	9.38	0.0024
ASQ	3.78993129	1.37340162	766.0576	7.61	0.0062
VSQ	2.26722928	1.37340162	274.1509	2.73	0.1000

THE ABOVE MODEL IS THE BEST 8 VARIABLE MODEL FOUND.

STEP 9 VARIABLE RT ENTERED

R SQUARE = 0.87969314

C(P) = 5.99225480

	DF	SUM OF SQUARES	MEAN SQUARE	F	PROB>F
REGRESSION	9	191051.97036661	21227.99671	211.24	0.0001
ERROR	260	26128.27321692	100.49336		
TOTAL	269	217180.24358354			

	B VALUE	STD ERROR	TYPE II SS	F	PROB>F
INTERCEPT	94.14540377				
RCS	37.02837394	0.91512002	164532.0572	1637.24	0.0001
ATKRALT	6.57003420	0.91512002	5179.8419	51.54	0.0001
VELSUM	-2.09781661	0.91512002	528.1001	5.26	0.0227
RT	-1.78938763	1.58503437	128.0763	1.27	0.2600
AV	-2.85012710	1.58503437	324.9290	3.23	0.0733
RSQ	-14.85938863	1.37268003	11776.0763	117.18	0.0001
TSQ	4.20722507	1.37268003	944.0396	9.39	0.0024
ASQ	3.78993129	1.37268003	766.0576	7.62	0.0062
VSQ	2.26722928	1.37268003	274.1509	2.73	0.0998

THE ABOVE MODEL IS THE BEST 9 VARIABLE MODEL FOUND.

STEP 10 VARIABLE RA ENTERED

R SQUARE = 0.87995403

C(P) = 7.43711555

	DF	SUM OF SQUARES	MEAN SQUARE	F	PROB>F
REGRESSION	10	191108.63157363	19110.86316	189.85	0.0001
ERROR	259	26071.61200991	100.66259		
TOTAL	269	217180.24358354			

	B VALUE	STD ERROR	TYPE II SS	F	PROB>F
INTERCEPT	94.14540377				
RCS	37.02837394	0.91589025	164532.0572	1634.49	0.0001
ATKRALT	6.57003420	0.91589025	5179.8419	51.46	0.0001
VELSUM	-2.09781661	0.91589025	528.1001	5.25	0.0228
RT	-1.78938763	1.58636845	128.0763	1.27	0.2604
RA	-1.19018073	1.58636845	56.6612	0.56	0.4538
AV	-2.85012710	1.58636845	324.9290	3.23	0.0736
RSQ	-14.85938863	1.37383538	11776.0763	116.99	0.0001
TSQ	4.20722507	1.37383538	944.0396	9.38	0.0024
ASQ	3.78993129	1.37383538	766.0576	7.61	0.0062
VSQ	2.26722928	1.37383538	274.1509	2.72	0.1001

THE ABOVE MODEL IS THE BEST 10 VARIABLE MODEL FOUND.

STEP 11 VARIABLE TV ENTERED

R SQUARE = 0.88003784

C(P) = 9.25879754

	DF	SUM OF SQUARES	MEAN SQUARE	F	PROB>F
REGRESSION	11	191126.83189652	17375.16654	172.06	0.0001
ERROR	258	26053.41168702	100.98222		
TOTAL	269	217180.24358354			

	B VALUE	STD ERROR	TYPE II SS	F	PROB>F
INTERCEPT	94.14540377				
RCS	37.02837394	0.91734316	164532.0572	1629.32	0.0001
ATKRALT	6.57003420	0.91734316	5179.8419	51.29	0.0001
VELSUM	-2.09781661	0.91734316	528.1001	5.23	0.0230
RT	-1.78938763	1.58888495	128.0763	1.27	0.2611
RA	-1.19018073	1.58888495	56.6612	0.56	0.4545
TV	-0.67454286	1.58888495	18.2003	0.18	0.6715
AV	-2.85012710	1.58888495	324.9290	3.22	0.0740
RSQ	-14.85938863	1.37601473	11776.0763	116.62	0.0001
TSQ	4.20722507	1.37601473	944.0396	9.35	0.0025
ASQ	3.78993129	1.37601473	766.0576	7.59	0.0063
VSQ	2.26722928	1.37601473	274.1509	2.71	0.1006

THE ABOVE MODEL IS THE BEST 11 VARIABLE MODEL FOUND.

STEP 12 VARIABLE TA ENTERED

R SQUARE = 0.88010686

C(P) = 11.11193508

	DF	SUM OF SQUARES	MEAN SQUARE	F	PROB>F
REGRESSION	12	191141.82165590	15928.48514	157.21	0.0001
ERROR	257	26038.42192764	101.31682		
TOTAL	269	217180.24358354			

	B VALUE	STD ERROR	TYPE II SS	F	PROB>F
INTERCEPT	94.14540377				
RCS	37.02837394	0.91886169	164532.0572	1623.94	0.0001
ATKRALT	6.57003420	0.91886169	5179.8419	51.13	0.0001
VELSUM	-2.09781661	0.91886169	528.1001	5.21	0.0232
RT	-1.78938763	1.59151513	128.0763	1.26	0.2619
RA	-1.19018073	1.59151513	56.6612	0.56	0.4552
TA	-0.61216336	1.59151513	14.9898	0.15	0.7008
TV	-0.67454286	1.59151513	18.2003	0.18	0.6720
AV	-2.85012710	1.59151513	324.9290	3.21	0.0745
RSQ	-14.85938863	1.37829254	11776.0763	116.23	0.0001
TSQ	4.20722507	1.37829254	944.0396	9.32	0.0025
ASQ	3.78993129	1.37829254	766.0576	7.56	0.0064
VSQ	2.26722928	1.37829254	274.1509	2.71	0.1012

THE ABOVE MODEL IS THE BEST 12 VARIABLE MODEL FOUND.

STEP 13 VARIABLE RV ENTERED

R SQUARE = 0.88014716

C(P) = 13.02616863

	DF	SUM OF SQUARES	MEAN SQUARE	F	PROB>F
REGRESSION	13	191150.57555081	14703.89043	144.61	0.0001
ERROR	256	26029.66803272	101.67839		
TOTAL	269	217180.24358354			

	B VALUE	STD ERROR	TYPE II SS	F	PROB>F
INTERCEPT	94.14540377				
RCS	37.02837394	0.92049982	164532.0572	1618.16	0.0001
ATKRALT	6.57003420	0.92049982	5179.8419	50.94	0.0001
VELSUM	-2.09781661	0.92049982	528.1001	5.19	0.0235
RT	-1.78938763	1.59435246	128.0763	1.26	0.2628
RA	-1.19018073	1.59435246	56.6612	0.56	0.4561
RV	0.46781126	1.59435246	8.7539	0.09	0.7694
TA	-0.61216336	1.59435246	14.9898	0.15	0.7013
TV	-0.67454286	1.59435246	18.2003	0.18	0.6726
AV	-2.85012710	1.59435246	324.9290	3.20	0.0750
RSQ	-14.85938863	1.38074973	11776.0763	115.82	0.0001
TSQ	4.20722507	1.38074973	944.0396	9.28	0.0026
ASQ	3.78993129	1.38074973	766.0576	7.53	0.0065
VSQ	2.26722928	1.38074973	274.1509	2.70	0.1018

THE ABOVE MODEL IS THE BEST 13 VARIABLE MODEL FOUND.

STEP 14 VARIABLE TGTALT ENTERED

R SQUARE = 0.88015946

C(P) = 15.00000000

	DF	SUM OF SQUARES	MEAN SQUARE	F	PROB>F
REGRESSION	14	191153.24649549	13653.80332	133.77	0.0001
ERROR	255	26026.99708804	102.06666		
TOTAL	269	217180.24358354			

	B VALUE	STD ERROR	TYPE II SS	F	PROB>F
INTERCEPT	94.14540377				
RCS	37.02837394	0.92225564	164532.0572	1612.01	0.0001
TGTALT	0.14919072	0.92225564	2.6709	0.03	0.8716
ATKRALT	6.57003420	0.92225564	5179.8419	50.75	0.0001
VELSUM	-2.09781661	0.92225564	528.1001	5.17	0.0238
RT	-1.78938763	1.59739362	128.0763	1.25	0.2637
RA	-1.19018073	1.59739362	56.6612	0.56	0.4569
RV	0.46781126	1.59739362	8.7539	0.09	0.7699
TA	-0.61216336	1.59739362	14.9898	0.15	0.7019
TV	-0.67454286	1.59739362	18.2003	0.18	0.6732
AV	-2.85012710	1.59739362	324.9290	3.18	0.0756
RSQ	-14.85938863	1.38338346	11776.0763	115.38	0.0001
TSQ	4.20722507	1.38338346	944.0396	9.25	0.0026
ASQ	3.78993129	1.38338346	766.0576	7.51	0.0066
VSQ	2.26722928	1.38338346	274.1509	2.69	0.1025

THE ABOVE MODEL IS THE BEST 14 VARIABLE MODEL FOUND.

D.3 ANOVA and Residual Plots

DEP VARIABLE: RNG

ANALYSIS OF VARIANCE

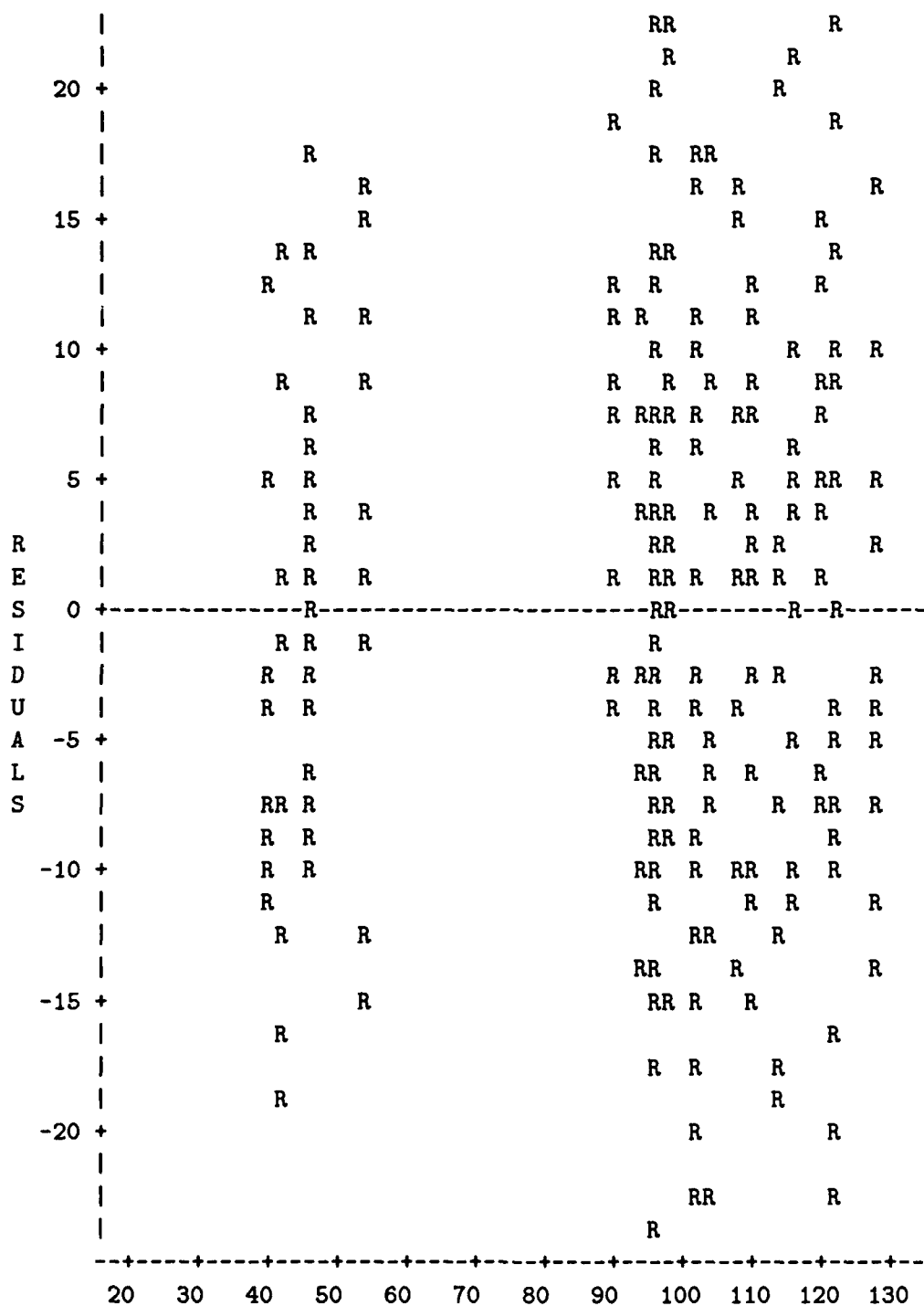
SOURCE	DF	SUM OF SQUARES	MEAN SQUARE	F VALUE	PROB>F
MODEL	6	190324.81421	31720.80237	310.647	0.0001
ERROR	263	26855.42938	102.11189877		
C TOTAL	269	217180.24358			
ROOT MSE		10.10504	R-SQUARE	0.8763	
DEP MEAN		92.10318	ADJ R-SQ	0.8735	
C.V.		10.97144			

PARAMETER ESTIMATES

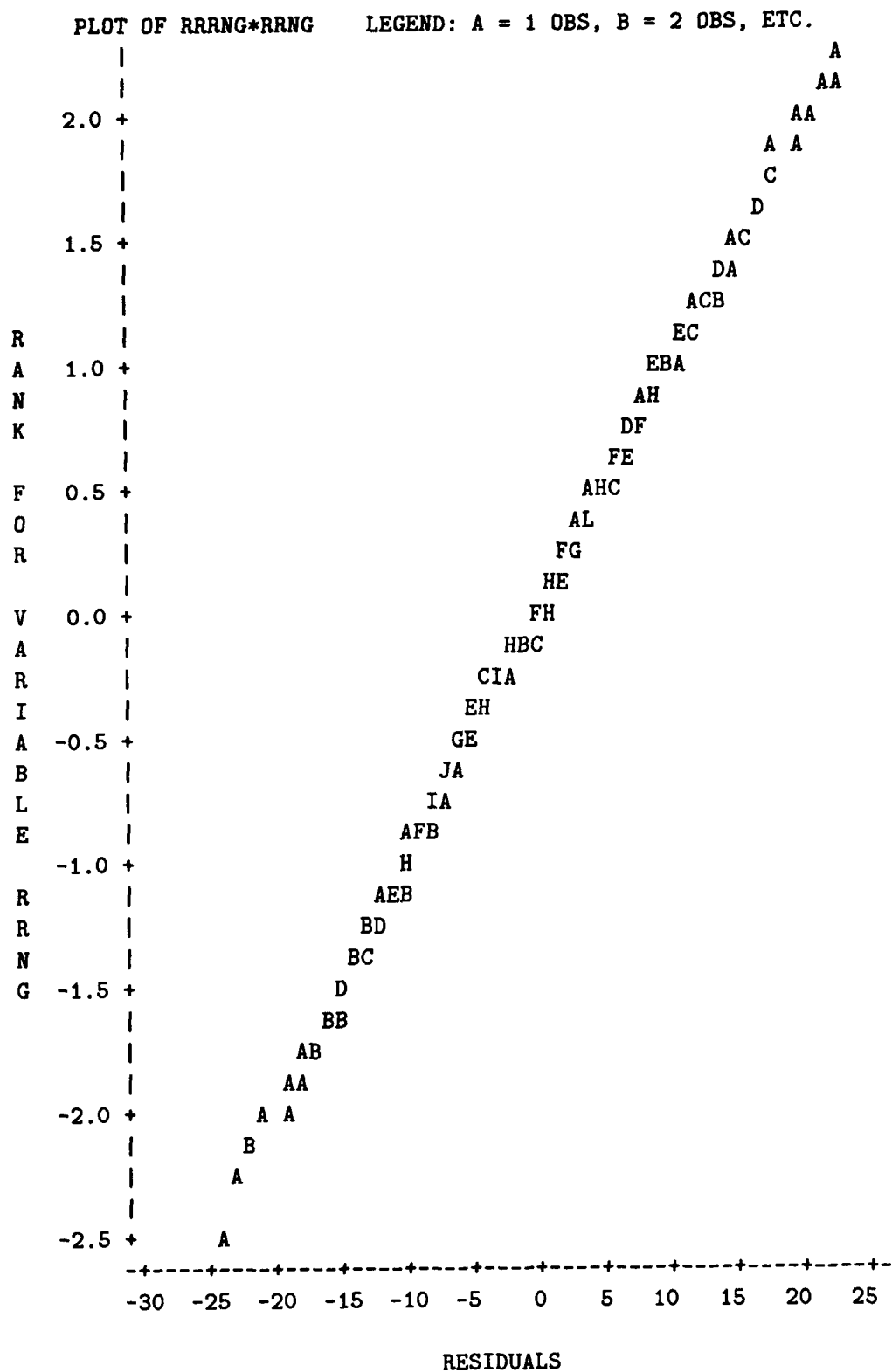
VARIABLE	DF	PARAMETER ESTIMATE	STANDARD ERROR	T FOR HO: PARAMETER=0
INTERCEP	1	96.16071868	1.37512221	69.929
RCS	1	37.02837394	0.92246002	40.141
ATKRALT	1	6.57003420	0.92246002	7.122
VELSUM	1	-2.09782	0.92246002	-2.274
RSQ	1	-15.6151	1.30455547	-11.970
TSQ	1	3.45148197	1.30455547	2.646
ASQ	1	3.03418819	1.30455547	2.326

VARIABLE	DF	PROB > T
INTERCEP	1	0.0001
RCS	1	0.0001
ATKRALT	1	0.0001
VELSUM	1	0.0238
RSQ	1	0.0001
TSQ	1	0.0086
ASQ	1	0.0208

PLOT OF RRNG*RNHAT SYMBOL USED IS R



NOTE: 76 OBS HIDDEN



Bibliography

1. 56TTW/DO/OTD (F-16 OTD TEAM), MacDill AFB, FL, *Air-to-Air Phase Manual, F-16*, APRIL 1983.
2. R. Browning. Lt Col. Chief, Campaign Branch. Telephone Interview. AFCSA/SAGFC, Pentagon, VA, 6 February 1989.
3. R. M. Page, *The Origin of Radar*. Garden City, MA: Ancho Books Doubleday & Co., Inc., 1962.
4. M. I. Skolnik, *Introduction to Radar Systems*. New York: McGraw-Hill Book Co., 1980.
5. G. W. Stimson, *Introduction to Airborne Radar*. El Segundo, CA: Hughes Aircraft Co., 1983.
6. D. K. Barton, *Modern Radar System Analysis*. Norwood, MA: Artech House, Inc., 1988.
7. N. E. Bent *et al.*, "The TAC BRAWLER Air Combat Simulation Analysts Manual, Rev. 5.0," Interim Report 906, Decision-Sciences Applications, Inc., Arlington, VA, June 1988.
8. G. E. P. Box and N. R. Draper, *Empirical Model-Building and Response Surfaces*. New York: John Wiley & Sons, 1987.
9. G. E. P. Box and D. W. Behnken, "Some New Three Level Designs for the Study of Quantitative Variables," *Technometrics*, vol. 6, pp. 455-475, November 1960.
10. N. R. Draper and H. Smith, *Applied Regression Analysis*. Norwood, MA: Artech House, Inc., second ed., 1988.

UNCLASSIFIED

SECURITY CLASSIFICATION OF THIS PAGE

REPORT DOCUMENTATION PAGE

Form Approved
OMB No. 0704-0188

1a. REPORT SECURITY CLASSIFICATION UNCLASSIFIED			1b. RESTRICTIVE MARKINGS		
2a. SECURITY CLASSIFICATION AUTHORITY			3. DISTRIBUTION / AVAILABILITY OF REPORT Approved for public release; distribution unlimited		
2b. DECLASSIFICATION / DOWNGRADING SCHEDULE					
4. PERFORMING ORGANIZATION REPORT NUMBER(S) AFIT/GST/ENS/89M-12			5. MONITORING ORGANIZATION REPORT NUMBER(S)		
6a. NAME OF PERFORMING ORGANIZATION School of Engineering		6b. OFFICE SYMBOL (If applicable) AFIT/ENS		7a. NAME OF MONITORING ORGANIZATION	
6c. ADDRESS (City, State, and ZIP Code) Air Force Institute of Technology (AU) Wright-Patterson AFB, Ohio 45433-6583			7b. ADDRESS (City, State, and ZIP Code)		
8a. NAME OF FUNDING / SPONSORING ORGANIZATION AFCSA/SAGE		8b. OFFICE SYMBOL (If applicable) SAGFC		9. PROCUREMENT INSTRUMENT IDENTIFICATION NUMBER	
8c. ADDRESS (City, State, and ZIP Code) Pentagon Washington DC 20330			10. SOURCE OF FUNDING NUMBERS		
			PROGRAM ELEMENT NO.	PROJECT NO.	TASK NO.
11. TITLE (Include Security Classification) A METHODOLOGY FOR MODELING RADAR DETECTION RANGE IN AIR COMBAT SIMULATION (UNCLASSIFIED)					
12. PERSONAL AUTHOR(S) Damon N. Lum, Major, USAF					
13a. TYPE OF REPORT MS Thesis		13b. TIME COVERED FROM _____ TO _____		14. DATE OF REPORT (Year, Month, Day) 1989 March	
15. PAGE COUNT 72					
16. SUPPLEMENTARY NOTATION					
17. COSATI CODES			18. SUBJECT TERMS (Continue on reverse if necessary and identify by block number) Radar, Radar Detection Range, Response Surface Methodology		
FIELD	GROUP	SUB-GROUP			
17	09				
12	03				
19. ABSTRACT (Continue on reverse if necessary and identify by block number) Advisor: Thomas F. Schuppe The purpose of this thesis is to develop a methodology for modeling fighter aircraft radar detection range performance. Response surface methodology is used to form a meta-model of the TAC BRAWLER Air Combat Model. Using experimental design theory, detection range data was collected using TAC BRAWLER and regressed to develop an equation for predicting radar detection range. The resulting equation is valid for specific ranges of the target's radar cross section, altitude, and airspeed and the attacker's altitude and airspeed. <i>Keywords: Radar, Response Surface Methodology (RSM)</i>					
20. DISTRIBUTION / AVAILABILITY OF ABSTRACT <input checked="" type="checkbox"/> UNCLASSIFIED/UNLIMITED <input type="checkbox"/> SAME AS RPT. <input type="checkbox"/> DTIC USERS			21. ABSTRACT SECURITY CLASSIFICATION UNCLASSIFIED		
22a. NAME OF RESPONSIBLE INDIVIDUAL Lt Col Thomas F. Schuppe, Asst. Prof.			22b. TELEPHONE (Include Area Code) 513 255-3362		22c. OFFICE SYMBOL AFIT/ENS